3-1-2011

Discovery of the first τ Sco Analogues: HD 66665 and HD 63425.

V. Petit
West Chester University

D. Massa
Space Telescope Science Institute

W. Marcolinino
Observatorio Nacional-MCT

G. Wade
Royal Military College of Canada

Richard Ignace
East Tennessee State University

Citation Information

Petit, V.; Massa, D.; Marcolinino, W.; Wade, G.; and Ignace, Richard. 2011. Discovery of the first τ Sco Analogues: HD 66665 and HD 63425.. *Monthly Notices Letters of the Royal Astronomical Society*. Vol.412(1). https://doi.org/10.1111/j.1745-3933.2010.01002.x ISSN: 1745-3933

Discovery of the first τ Sco Analogues: HD 66665 and HD 63425.

Monthly Notices of the ROYAL ASTRONOMICAL SOCIETY LETTERS

Mon. Not. R. Astron. Soc. **412,** L45–L49 (2011) doi:10.1111/j.1745-3933.2010.01002.x

Discovery of the first τ Sco analogues: HD 66665 and HD 63425⋆

V. Petit,[1]† D. L. Massa,[2] W. L. F. Marcolino,[3] G. A. Wade,[4] R. Ignace[5] and The MiMeS Collaboration

[1]*Department of Geology & Astronomy, West Chester University, West Chester, PA 19383, USA*
[2]*Space Telescope Science Institute, 3700 N. San Martin Drive, Baltimore, MD 21218, USA*
[3]*Observatório Nacional-MCT, Rua José Cristino, 77, CEP 20921-400, São Cristóvão, Rio de Janeiro, Brazil*
[4]*Department of Physics, Royal Military College of Canada, PO Box 17000, Station Forces, Kingston, ON K7K 4B4, Canada*
[5]*Department of Physics & Astronomy, East Tennessee State University, Box 70652, Johnson City, TN 37614, USA*

Accepted 2010 December 17. Received 2010 December 16; in original form 2010 October 30

ABSTRACT

The B0.2 V magnetic star τ Sco stands out from the larger population of massive OB stars due to its high X-ray activity, peculiar wind diagnostics and highly complex magnetic field. This Letter presents the discovery of the first two τ Sco analogues – HD 66665 and HD 63425, identified by the striking similarity of their ultraviolet (UV) spectra to that of τ Sco. ESPaDOnS spectropolarimetric observations were secured by the Magnetism in Massive Stars CFHT Large Program, in order to characterize the stellar and magnetic properties of these stars. CMFGEN modelling of optical ESPaDOnS spectra and archived *IUE* UV spectra showed that these stars have stellar parameters similar to those of τ Sco. A magnetic field of similar surface strength is found on both stars, reinforcing the connection between the presence of a magnetic field and wind peculiarities. However, additional phase-resolved observations will be required in order to assess the potential complexity of the magnetic fields and verify if the wind anomalies are linked to this property.

Key words: stars: early-type – stars: magnetic field.

1 THE MAGNETIC B-TYPE STAR τ SCO

Very little is known about the magnetic fields of hot, massive OB stars. Due at least in part to the challenges of measurement, direct evidence of magnetic fields in massive stars is remarkably rare – there are perhaps 30 known examples – and few have been studied in detail.

Even as a member of the elusive class of magnetic massive stars, the B0.2 V star τ Sco is recognized to be a peculiar and outstanding object. First, τ Sco is distinguished by its magnetic field, which is unique, because it is structurally far more complex than the mostly dipolar (multipole mode $l = 1$) fields usually observed in magnetic OB stars. According to the Zeeman Doppler Imaging performed by Donati et al. (2006), the magnetic topology of τ Sco presents significant power in multipole modes up to $l = 5$ with a mean surface field strength of $\sim$300 G and the extrapolated 3D field structure shows an intricate assortment of open field lines and closed magnetic loops (illustrated in figs 11 and 12 of Donati et al. 2006).

Secondly, τ Sco also stands out from the crowd of early-B stars because of its stellar wind anomalies, as diagnosed through its odd ultraviolet (UV) spectrum and X-ray emission. The optical and non-resonance UV lines of τ Sco that probe the conditions of the photosphere are typical of an early-B dwarf star. However, the UV resonance lines arising from the stellar wind are not those typical of such a star. Fig. 1 shows a comparison of the UV spectrum of τ Sco (second spectrum) with the spectrum of a normal B0 main-sequence star (bottom spectrum) and a B0 giant (top spectrum). The resonance wind lines of C IV (right-hand panel), and Si IV and N V (left-hand panel) are indicated with the dashed lines. The UV wind line morphology of normal, early-B stars conforms to a 2D spectral grid (Walborn, Parker & Nichols 1995). Typically, C IV strengthens with increasing temperature and luminosity. N V is very weak on the main sequence at spectral type B0 V but strengthens with temperature and luminosity. For stars with fixed C IV and N V profiles, Si IV is strictly luminosity-dependent and breaks the degeneracy. τ Sco does not fit into this grid. It has strong N V indicating that it should be well above the main sequence. However, its C IV lines are only slightly stronger than typical and not distinctly wind-like, suggesting a near-main-sequence luminosity. Finally, its Si IV profiles are unique, a bit stronger than typical class V stars, but unlike normal, early giants. As a result, this star lies outside the normal classification grid, suggesting a more highly ionized outflow than typical. The hard X-ray emission of τ Sco also suggests hot plasma,

⋆Based on observations obtained at the Canada–France–Hawaii Telescope (CFHT) which is operated by the National Research Council of Canada, the Institut National des Sciences de l'Univers of the Centre National de la Recherche Scientifique of France and the University of Hawaii.

†E-mail: VPetit@wcupa.edu

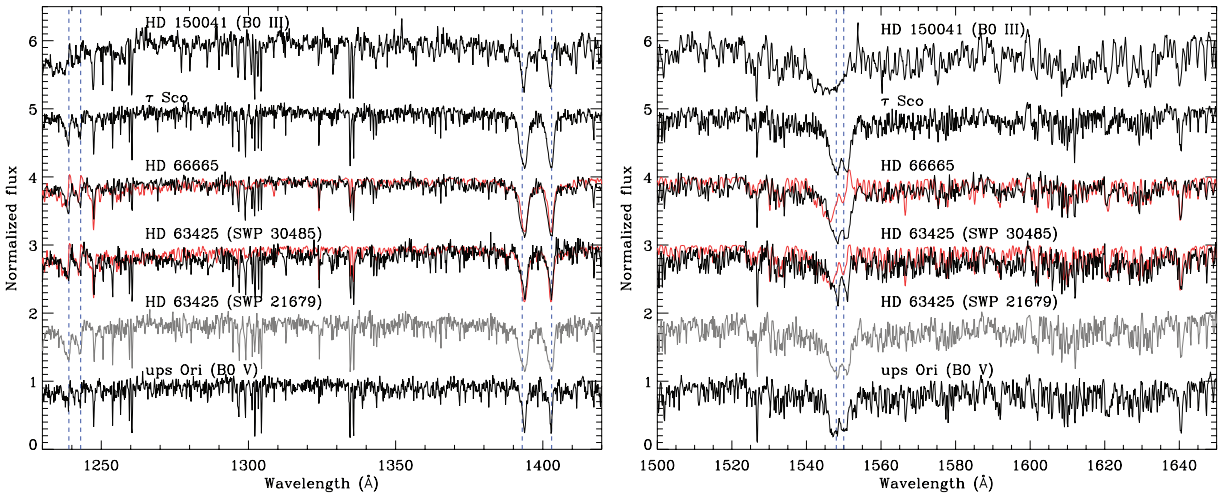

Figure 1. *IUE* spectra of τ Sco and its analogues HD 66665 and HD 63425 (second to fifth spectra). For comparison, typical spectra of a B0 dwarf and a B0 giant are shown (bottom and top, respectively). The dashed lines indicate the wind lines N V $\lambda\lambda$1239, 1243, Si IV $\lambda\lambda$1393, 1403 and C IV $\lambda\lambda$1548, 1550. The best-fitting synthetic spectra, from which stellar parameters were derived, for HD 66665 and HD 63425, are shown in red.

in excess of 10 MK (Cassinelli et al. 1994). We suspect that this is connected to the strange UV properties. Like its magnetic field, the stellar wind of τ Sco possesses observational characteristics that make it unique among OB stars.

Interestingly, the wind lines of τ Sco have been shown to vary periodically with the star's 41 d rotation period (Donati et al. 2006), which is interpreted to mean that the wind is structured and modulated by the magnetic field. Clearly, the magnetic field exerts an important influence on the wind dynamics. What is not clear is whether the wind-line anomalies described above are a consequence of the unusual complexity of τ Sco's magnetic field, a general consequence of wind confinement in this class of stars, or perhaps even unrelated to the presence of a magnetic field. Because such wind anomalies have never been observed in any other star, magnetic or not, this issue has remained unresolved.

The identification and analysis of additional stars with wind properties similar to τ Sco would therefore represent an important step towards understanding the origin of these peculiarities. In this Letter, we present two early-B-type stars – HD 66665 and HD 63425 – that we identified to be the first τ Sco analogues based on their UV spectra, which are strikingly similar to the UV spectrum of τ Sco. Fig. 1 shows *IUE* archive spectra of these two stars (third to fifth spectra from the top). The discovery of wind anomalies naturally led to an investigation of the magnetic properties of these stars by the Magnetism in Massive Stars (MiMeS) collaboration (Wade et al. 2011).

2 OBSERVATIONS

Spectropolarimetric observations of HD 66665 and HD 63425 were obtained with the ESPaDOnS at the Canada–France–Hawaii Telescope (CFHT). We acquired four high-resolution ($R \sim 65\,000$) broad-band (370–1050 nm) intensity (Stokes I) and circular polarization (Stokes V) spectra for each star, during about 10 consecutive nights in 2010 February/March. A summary of the ESPaDOnS observations is given in Table 1. For a complete description of the observation procedure and reduction procedure with the LIBRE-ESPRIT package provided by the CFHT, see Donati et al. (1997). In addition to the ESPaDOnS observations, the available archival *IUE* spectra are also listed in Table 1.

Table 1. Journal of ESPaDOnS observations listing the UT date, the heliocentric Julian date (240 0000+), the total exposure time and the S/N per 1.8 km s^{-1} velocity bin at 540 nm. Column 5 gives the probability that the observed signal in Stokes V LSD profiles is due only to noise and column 6 gives the global longitudinal field component obtained from the first moment of the Stokes V profiles. The available archival *IUE* spectra are also listed.

Date (UT)	HJD	$t_{\rm exp}$ (s)	S/N	FAP	$B_l{}^a$ (G)
		HD 66665			
2010/02/26	552 53.97	4400	728	$<10^{-8}$	-93 ± 4
2010/03/02	552 57.98	1200	236	$<10^{-8}$	-3 ± 15
2010/03/04	552 59.98	1200	330	$<10^{-8}$	9 ± 10
2010/03/05	552 60.98	1200	276	2×10^{-6}	41 ± 13
1983/12/04	454 36.77	900		*IUE* swp 21680	
1987/03/11	468 66.49	420		*IUE* swp 30484	
1987/03/12	468 66.58	1080		*IUE* swp 30486	
		HD 63425			
2010/02/28	552 55.84	1200	520	$<10^{-8}$	117 ± 8
2010/03/03	552 58.88	1200	289	$<10^{-8}$	113 ± 15
2010/03/07	552 62.76	1200	435	$<10^{-8}$	132 ± 10
2010/03/08	552 63.83	1200	361	$<10^{-8}$	125 ± 12
1987/03/12	468 66.53	600		*IUE* swp 21679	
1983/12/04	456 72.74	720		*IUE* swp 30485	

[a] A detectable Stokes V signal can be observed with high-resolution instruments even if the global longitudinal field is null (see Petit 2011).

3 STELLAR PARAMETERS

In order to determine the stellar and wind parameters of HD 66665 and HD 63425, we used non-local thermodynamic equilibrium model atmospheres and spectrum synthesis from the CMFGEN code. CMFGEN solves for the radiative transfer equation in a spherically symmetric outflow together with the radiative and statistical equilibrium equations, taking into account effects such as line-blanketing and X-rays (for details, see Hillier & Miller 1998).

We used optical spectra to derive the surface gravity ($\log g$) and effective temperature ($T_{\rm eff}$), using classic line diagnostics (i.e. Balmer line wings and He I–He II lines). UV spectra from the *IUE* were used to infer stellar wind properties. All results are summarized in

Table 2. Summary of stellar properties of τ Sco, HD 66665 and HD 63425.

	τ Sco[a]	HD 66665	HD 63425
Spectral type	B0.2 V	B0.5 V	B0.5 V
$T_{\rm eff}$ (kK)	31 ± 1	28.5 ± 1.0	29.5 ± 1.0
$\log g$ (cgs)	4.0 ± 0.1	3.9 ± 0.1	4.0 ± 0.1
$R_\star$ ($R_\odot$)	5.6 ± 0.8	$5.5^{+3.3}_{-2.7}$	$6.8^{+4.8}_{-2.0}$
$\log (L_\star/L_\odot)$	4.47 ± 0.13	$4.25^{+0.40}_{-0.60}$	$4.50^{+0.46}_{-0.30}$
$M_\star$ ($M_\odot$)	11 ± 4	9^{+5}_{-7}	17^{+34}_{-9}
$v \sin i$ (km s^{-1})	<13	$\lesssim$10	$\lesssim$15
$\dot{M}$ (10^{-9} $M_\odot$ yr^{-1})	61^{+10}_{-2}	<0.45	<0.75
v_∞ (km s^{-1})	∼2000	∼1400	∼1700

[a]Parameters from Simón-Díaz et al. (2006) and Mokiem et al. (2005) for $\dot{M}$ and v_∞.

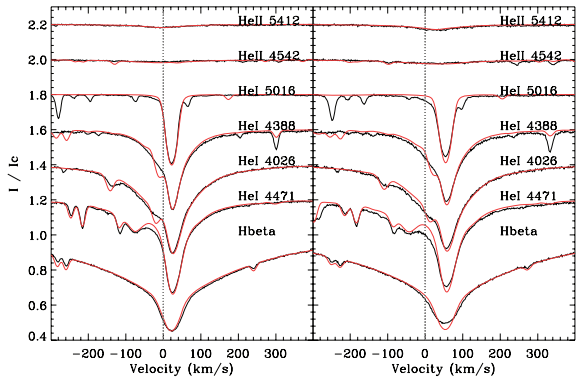

Figure 2. Fits to the optical He I–He II and Hβ lines for HD 66665 (left-hand frame) and HD 63425 (right-hand frame).

Table 2, along with those of τ Sco for comparison. A solar chemical composition was adopted, following Asplund et al. (2009). We postpone a detailed analysis regarding chemical abundances for a future study.

3.1 HD 66665

The various estimates for the distance of HD 66665 range from about 1 to 2 kpc (Savage et al. 1985; Savage & Massa 1987; Diplas & Savage 1994; van Leeuwen 2007). We adopted an intermediate value of 1.5 kpc and assumed an uncertainty of a factor of 2.[1] The stellar luminosity $L_\star$ was then derived by fitting the spectral energy distribution using the *IUE* spectrum and *UBVJHK* photometry, converted to flux points. An $E(B-V) = 0.02$ and $R = 3.1$ were used to fit the observed data (Diplas & Savage 1994). The stellar radius ($R_\star$) and mass ($M_\star$) follow directly from the chosen $L_\star$, $T_{\rm eff}$ and $\log g$.

A very good agreement is obtained for the optical diagnostic lines in HD 66665. In Fig. 2 (left-hand frame), we present fits to different He I–He II lines and Hβ. Our model was convolved with a $v \sin i$ of 8 km s^{-1}. We, however, note that this value is an estimate. Values in excess of 10 km s^{-1} tend to produce profiles which are generally broader than the ones observed, but accurate lower values are difficult to determine. No significant variability was observed in the optical spectra of HD 66665.

The UV spectrum of HD 66665 was first pointed out as unusual by Grigsby (1992). The absorption shown by C IV cannot be reproduced in detail by our models (see Fig. 1). Several tests were performed, but the observed profile is always too deep compared to the synthetic ones. On the other hand, we could achieve an acceptable fit for the Si IV and N V lines. The inclusion of X-rays in our CMFGEN models was essential in producing the N V feature, since the wind structure is not sufficiently ionized without this component.

Despite the problem found for C IV, we could derive an upper limit for the mass-loss rate ($\dot{M}$) from the emission part of the synthetic P-Cygni profile of the same line. When $\dot{M}$ is greater than about 4.5×10^{-10} $M_\odot$ yr^{-1}, the model predicts a relatively strong P-Cygni emission which is clearly absent in the observed spectrum, as it is in the spectrum of τ Sco. Furthermore, only a rough estimate for the wind terminal velocity ($v_\infty \simeq 1\,400$ km s^{-1}) could be made.

3.2 HD 63425

We adopted a distance to HD 63425 of 1136 pc (from $\pi = 0.88 \pm 0.36$ mas; van Leeuwen 2007). The stellar luminosity was then derived in the same way as in HD 66665. For the reddening parameters, we use $R = 3.1$ and $E(B-V) = 0.10$ (Savage & Massa 1987). Our fits to the He I–He II diagnostic lines and Hβ are presented in Fig. 2 (right-hand frame). The optical spectra of HD 63425 and HD 66665 are similar. However, our analysis indicates a slightly higher effective temperature and surface gravity for HD 63425. Moreover, Balmer line cores in HD 63425 are shallower, especially Hα and Hβ. Line filling by a much higher mass-loss rate than the one in our final model is not a reasonable explanation here, since it would produce strong UV wind profiles which are not observed. A possible explanation for this line filling could be contamination (emission) from material trapped by the magnetic field, distinct from the outflowing wind. This problem does not occur in HD 66665, where we have good fits to entire Balmer line profiles.

The apparent rotational velocity of HD 63425 is low, but an accurate value is difficult to infer from the observed spectrum. Values above 15 km s^{-1} tend to produce profiles that are broader than the ones observed. After various tests, we adopted $v \sin i$ of 11 km s^{-1} for the convolution of our final model.

There are only two *IUE* spectra of HD 63425. Interestingly, although the optical spectra of HD 63425 do not show any variation, these UV spectra (obtained over 3 years apart) reveal large variations in the wind lines (see the two spectra shown in Fig. 1). The SWP 21679 spectrum presents these features larger and deeper than the ones found in SWP 30485. An interesting possibility was proposed to explain a similar issue in the star τ Sco. The passage of the magnetic equator across the line of sight would reveal material trapped by the magnetic field, providing the extra absorption observed (Donati et al. 2006). Unfortunately, given the scarcity of UV data for HD 63425, we have no means to test this idea at present (e.g. by verifying the existence of absorption episodes).

We chose to focus on the SWP 30485 spectrum, where we have shallower absorption profiles. Nevertheless, the mass-loss rate obtained can be safely used as an upper limit. Our fit is illustrated in Fig. 1. Again, the use of X-rays was mandatory in producing an N V feature comparable to the observed one. We note that the C IV λλ1548, 1550 absorptions could be partially or entirely due to the interstellar medium. We summarize the wind parameters obtained in Table 2, which are similar to those of HD 66665.

4 MAGNETIC FIELD

In order to increase the magnetic sensitivity of our data, we applied the least-squares deconvolution (LSD) procedure, as described by

[1] Note that the recently revised parallax for HD 66665 is very uncertain, namely, $\pi = -0.94 \pm 1.05$ mas (van Leeuwen 2007).

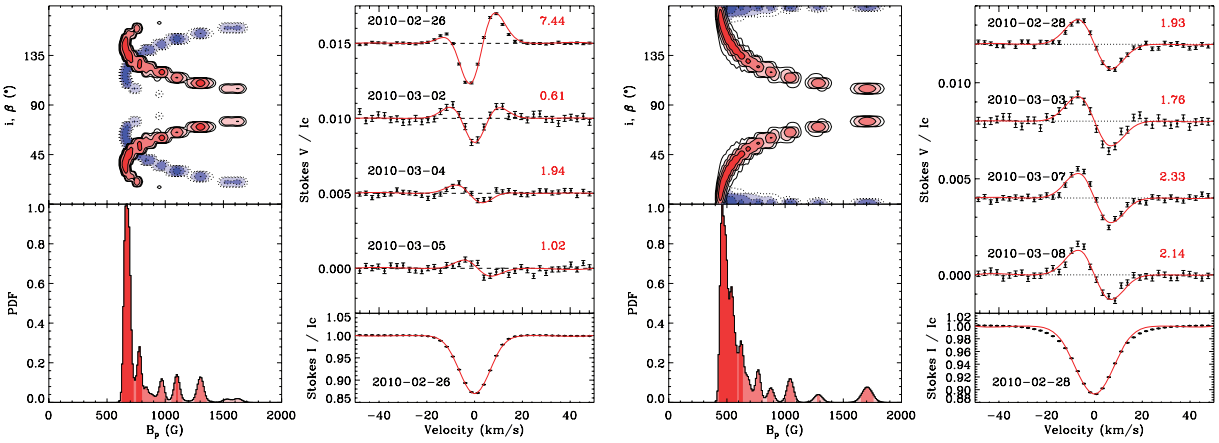

Figure 3. Magnetic modelling of HD 66665 (left-hand panel) and HD 63425 (right-hand panel). For each star, the left-hand panel shows the posterior probability density marginalized for the dipole strength B_p (bottom), and for the 2D B_p–i (solid red) and B_p–β (dashed blue) planes (top). The credible regions containing 68.3, 95.4, 99 and 99.7 per cent of the probability are shaded, from dark to light colours, respectively. The right-hand panel shows the LSD Stokes I profile for one observation (bottom) and all LSD Stokes V profiles (top). The synthetic profiles produced by the (B_p, i, β) configuration correspond to the peak of the joint posterior probability density, the best phase being extracted for each observation. The corresponding χ^2_{red} is indicated.

Donati et al. (1997). This procedure enables the simultaneous use of many lines present in a spectrum to detect a magnetic field Stokes V signature. Assumptions, limitations and numerical tests of this method are presented by Kochukhov, Makaganiuk & Piskunov (2010).

We adopted lists of metallic spectral lines suitable for early-B stars from the Vienna Atomic Line Data base (Kupka et al. 2000). The depth of each line was adjusted to match the observed spectra of each star. In total, around 300 and 260 lines were used for HD 66665 and HD 63425, respectively. All LSD profiles were computed on a spectral grid with a velocity bin of 2.6 km s^{-1}.

In order to assess the presence of a magnetic signature in our LSD profiles, we computed the χ^2 probability that the observed deviation of the signal, with respect to $V = 0$, is only due to noise (the false alarm probability or FAP). We consider a signal to be detected when this probability is less than 10^{-5}, as prescribed by Donati et al. (1997). As shown in column 5 of Table 1, all observations led to the detection of a magnetic signal. The same analysis was performed on the diagnostic null (N) profiles, where no signals were detected.

The global longitudinal component of the magnetic field was inferred from the first moment of each Stokes V LSD profile, as described by Wade et al. (2000). The integration range on each side of the Stokes I centre of gravity was set to $\pm$22 and $\pm$25 km s^{-1} for HD 66665 and HD 63425, respectively. While the longitudinal field provides a useful statistical measure of the line-of-sight component of the field, we stress that we do not use it as the primary diagnostic of the presence of a magnetic field. This is because a large variety of magnetic configurations can produce a null longitudinal field while still generating a detectable Stokes V profile in the velocity-resolved line profiles (see Petit 2011).

Fig. 3 (left-hand panel, right-hand frame) shows the LSD profiles of HD 66665. The Stokes V profiles vary on a time-scale of at most a few days, although a period determination is not possible at this point. As the exact rotation phases of our observations are not known, we used the method described by Petit et al. (2008), which compares the observed Stokes V profiles to a large grid of synthetic profiles, described by a dipole oblique rotator model. The model is parametrized by the dipole field strength B_p, the rotation axis inclination i with respect to the line of sight, the positive magnetic axis obliquity β and the rotational phase φ. Assuming that only φ may change between different observations of a given star, the goodness-of-fit of a given rotation-independent (B_p, i, β) magnetic configuration can be computed to determine configurations that provide good posterior probabilities for all the observed Stokes V profiles, in a Bayesian statistic framework.

In Fig. 3 (left-hand panel, right-hand frame), we show the synthetic profiles (in solid red) produced by the (B_p, i, β) configuration that produces the peak of the joint posterior probability. The inclined dipole model can reproduce the current observations in a satisfactory fashion, although χ^2_{red} remains high for two observations [those with the highest signal-to-noise ratio (S/N)]. Whether these deviations from the model come from artefacts of the LSD procedure, systematics introduced by our simple line-profile modelling or a more complex field remains to be investigated, once phase-resolved observations are obtained and a more detailed analysis can be performed.

By treating any features that cannot be explained by the inclined dipole model as additional Gaussian noise, we can obtain a conservative estimate of the model parameters. For HD 66665, the posterior probability density marginalized for B_p (Fig. 3, left-hand panel, left-hand frame) peaks at 670 G and provides a strong constraint on the dipole field lower limits (606 G at 99.7 per cent). However, the probability density function (PDF) extends to high B_p (1.6 kG at 99.7 per cent), as the exact field strength depends strongly on the geometry, as illustrated by the 2D PDFs, marginalized for the B_p–i and B_p–β planes.

The LSD profiles obtained for HD 63425 are shown in Fig. 3 (right-hand panel, right-hand frame). No significant variations are observed between the profiles. The red curves show the synthetic profiles produced by the (B_p, i, β) configuration that produces the peak of the joint posterior probability. The inclined dipole model can once again reproduce the current observations in a satisfactory fashion, although some details are not reproduced, as shown by the χ^2_{red} values. Note that our simple modelling of the Stokes I profile was not able to reproduce the broad wings of the intensity line profile. The posterior probability density marginalized for B_p (right-hand panel, left-hand frame) peaks at 460 G, and the 99.7 per cent credible region extends from 406 G to 1.8 kG, depending on the exact geometry. As no assumptions are made about the phases

of each observation, the model prefers a dipole field that is roughly aligned with the rotation axis ($\beta \sim 0^\circ$), as this configuration is more likely to occur with observations taken at random rotational phases. However, given the low $v \sin i$ and the short time-span of our observations, it is possible that all our observations were taken at roughly the same rotational phase. This would suggest that the stellar rotation period is much longer than the period of the observations. Given the resemblance of this star with τ Sco, and the observed variability of the UV line profiles, this hypothesis is likely. More observations shall therefore be necessary to constrain the exact geometry of the field.

5 CONCLUSION

We have presented the characteristics of two stars – HD 66665 and HD 63425 – which we believe are analogues to the magnetic massive star τ Sco for two main reasons: (i) the UV spectra of these stars are similar to the once-unique spectrum of τ Sco; and (ii) we have shown that these two stars host magnetic fields.

We have shown that all three of these stars have similar fundamental properties. However, the mass-loss rates we estimate for HD 66665 and HD 63425 are lower than the value adopted for τ Sco by Donati et al. (2006, $6 \times 10^{-8}\,M_\odot\,yr^{-1}$) in their analysis of that star. However, that mass-loss rate (Mokiem et al. 2005) is determined from the optical spectrum of τ Sco and could differ systematically from that determined from UV line profiles – in particular in the presence of a magnetic field.

The derived mass-loss rates for HD 66665 and HD 63425 are sufficiently low that they should be considered as stars presenting the weak wind problem (Martins et al. 2005; Marcolino et al. 2009), since the expected mass-loss rate is about $10^{-8}\,M_\odot\,yr^{-1}$ – about 20 times larger than the inferred rates (following the recipe provided by Vink, de Koter & Lamers 2000).

Our modelling of the LSD Stokes *V* profiles, assuming an inclined dipole model, results in surface field strengths[2] that are comparable to, or perharps slightly larger than, the mean surface field strength of τ Sco. The current observations can be acceptably reproduced by the dipole model, although more phase-resolved observations are required in order to assess the potential complexity of their magnetic fields and verify if the wind anomalies are linked to the field complexity.

[2] The surface averaged modulus of a dipolar magnetic field is equal to 0.77 times the dipole polar field strength.

ACKNOWLEDGMENTS

GAW acknowledges support from the Discovery Grants programme of the Natural Science and Engineering Research Council of Canada. We thank the anonymous referee whose helpful comments led to the improvement of this Letter.

REFERENCES

Asplund M., Grevesse N., Sauval A. J., Scott P., 2009, ARA&A, 47, 481
Cassinelli J. P. et al., 1994, ApJ, 421, 705
Diplas A., Savage B. D., 1994, ApJS, 93, 211
Donati J.-F. et al., 1997, MNRAS, 291, 658
Donati J.-F. et al., 2006, MNRAS, 370, 629
Grigsby J., 1992, BAAS, 24, 800
Hillier D. J., Miller D. L., 1998, ApJ, 496, 407
Kochukhov O., Makaganiuk V., Piskunov N., 2010, A&A, 524, A5
Kupka F. G. et al., 2000, Baltic Astron., 9, 590
Marcolino W. L. F. et al., 2009, A&A, 498, 837
Martins F. et al., 2005, A&A, 441, 735
Mokiem M. R. et al., 2005, A&A, 441, 711
Petit V., 2011, in Neiner C., Wade G., Meynet G., Peters G., eds, Proc. IAU Symp. 272, Active OB Stars. Cambridge Univ. Press, Cambridge, in press
Petit V., Wade G. A., Drissen L., Montmerle T., Alecian E., 2008, MNRAS, 387, L23
Savage B. D., Massa D., 1987, ApJ, 314, 380
Savage B. D., Massa D., Meade M., Wesselius P. R., 1985, ApJS, 59, 397
Simón-Díaz S., Herrero A., Esteban C., Najarro F., 2006, A&A, 448, 351
van Leeuwen F., 2007, A&A, 474, 653
Vink J. S., de Koter A., Lamers H. J. G. L. M., 2000, A&A, 362, 295
Wade G. A., Donati J.-F., Landstreet J. D., Shorlin S. L. S., 2000, MNRAS, 313, 851
Wade G. A. et al., 2011, in Neiner C., Wade G., Meynet G., Peters G., eds, Proc. IAU Symp. 272, Active OB Stars. Cambridge Univ. Press, Cambridge, in press
Walborn N. R., Parker J. W., Nichols J. S., 1995, NASA Reference Publication, 1363

This paper has been typeset from a TEX/LATEX file prepared by the author.